Wiley
Journal of Food Processing and Preservation
Volume 2026, Article ID 3563570, 16 pages
https://doi.org/10.1155/jfpp/3563570

WILEY

Research Article

Micro- and Macroscopic Analysis of Agglomerate-Driven Oil Immobilization in Nut-Based Pastes

Hilke Schacht,[1] **Lena Trapp**,[2] **Maike Föste**,[1] **Isabell Rothkopf**,[1] **and Gisela Guthausen**[2,3]

[1]*Department of Process Engineering, Fraunhofer Institute for Process Engineering and Packaging IVV, Freising, Germany*
[2]*Institute of Mechanical Process Engineering and Mechanics, Karlsruhe Institute of Technology, Karlsruhe, Germany*
[3]*Department of Water Chemistry and Technology, Engler-Bunte-Institut, Karlsruhe Institute of Technology, Karlsruhe, Germany*

Correspondence should be addressed to Hilke Schacht; hilke.schacht@ivv.fraunhofer.de

Received 21 July 2025; Revised 15 November 2025; Accepted 24 December 2025

Academic Editor: Poulami Jha

Oil mobility is a key determinant of stability in hazelnut-based pastes, as it promotes oil separation, which in turn causes a greasy texture and increased susceptibility to oxidation. It is hypothesized that (1) grinding leads to the formation of agglomerates that immobilize oil and thus prevent oil separation and that (2) mixing disrupts these structures, resulting in destabilization and increased oil mobility. The understanding of the formation, process dependency, and functional relevance of agglomerates is limited by the lack of analytical methods for their detection. This study employed a multiscale analytical approach combining microscopic techniques (light microscopy and NMR diffusometry) for direct detection of agglomerates with macroscopic measurements (oil binding capacity, rheology, and oil separation during 4 weeks of storage) to reveal their function in nut pastes of increasing complexity: pure hazelnut pastes (100% w/w nuts), hazelnut–sugar pastes (70% w/w nuts and 30% w/w sugar), and nougat formulations. Grinding technologies (cutter, ball mill, and roller refiner) at two intensities were compared during the production of pure hazelnut and hazelnut–sugar pastes. Based on these results, nougat pastes were produced at laboratory and industrial scales using roller refining. Mixing conditions of nougat pastes were varied to evaluate the stability of agglomerates and its impact on oil mobility. Agglomerate structures were detected using microscopic techniques, depending on processing technology, intensity, and composition of hazelnut-based pastes. In macroscopic tests, their presence was associated with enhanced oil immobilization and improved product stability. These findings demonstrate that oil mobility in hazelnut-based pastes is strongly influenced by grinding and mixing conditions and highlight the relevance of a multiscale analytical approach to optimize processing for stable fat-based products.

Keywords: agglomerates; grinding; hazelnut paste; mixing; nougat paste; oil diffusion; oil mobility; oil separation; processing

1. Introduction

Hazelnut-based pastes, such as nougat, are complex systems of different solid particles, such as sugar, roasted hazelnuts, and cocoa powder, dispersed in a continuous phase of oils and fats [1]. This continuous phase consists mainly of hazelnut oil, which is rich in unsaturated low-melting triacylglycerides (TAGs) such as triolein (2,3-bis[{(*Z*)-octadec-9-enoyl}oxy]propyl (*Z*)-octadec-9-enoate, $C_{57}H_{104}O_6$) [2]. These TAGs are liquid at room temperature and are thus highly mobile [3, 4]. Mobile oil can contribute to or accelerate oil separation on the surface of nut pastes, leading to a greasy texture and increased susceptibility to oxidation [5].

Earlier studies have addressed the impact of composition—such as fat-to-sugar ratios [1], sugar substitutes [6], and fat crystallization behavior [7–10]—on the stability of nut-based pastes. In contrast, the role of processing steps such as grinding and mixing and their contribution to oil immobilization through structural changes like formation of agglomerates has received little attention. In this study, agglomerates are operationally defined as densely packed, cohesive particle assemblies that entrap or retain oil inside.

It is hypothesized that grinding—especially by roller refining—leads to the formation of agglomerates that entrap oil and thus prevent oil separation. Roller refiners exert high compressive forces, especially at fine settings, where particles may be compacted into dense structures capable of immobilizing oil [11–13]. In contrast, cutters or beater blade mills are typically used for pregrinding or for processing semisolid materials, such as natural sugar replacers like dates. They primarily apply shear forces, resulting in coarser particles with minimal compressive stress [14, 15]. Ball mills combine shear, compression, and impact forces, producing finer but loosely packed structures. Simultaneously, they enable continuous mixing, during which particles are broken down and coated with fat, potentially limiting direct particle–particle interactions [16–18].

It is further hypothesized that subsequent mixing steps—typically performed using conches, anchor stirrers, or planetary mixers in nut paste production—disrupt agglomerates by applying shear stress, potentially causing their destabilization and oil release [19].

This study is aimed at investigating how grinding and mixing conditions affect oil immobilization in hazelnut-based pastes. A multiscale analytical approach was applied to identify agglomerates with entrapped oil microscopically and to assess their functional role using macroscopic analyses.

Initially, the impact of grinding technology (cutter, ball mill, or roller refiner) and intensity (two levels) was evaluated using pure hazelnut pastes (100% w/w nut) and hazelnut–sugar pastes (70% w/w nut and 30% w/w sugar). Based on these findings, nougat pastes—consisting of an even more complex compositional matrix—with three grinding degrees (Gs) (coarse, medium, and fine) were produced at laboratory and industrial scales using roller refining for medium and fine grinding, since only this technology provided clear evidence of agglomerate formation. Nougat pastes were further subjected to varying mixing durations (MDs) and mixing temperatures (MTs) to evaluate agglomerate stability.

At the microstructural level, light microscopy and NMR diffusion measurements were used to detect agglomerates with entrapped oil. Complementary macroscopic tests—including oil binding capacity (OBC), rheology, and oil separation during 4 weeks of storage—provided indirect functional indicators of agglomerate presence under varying processing conditions, enabling a differentiated evaluation of structural and functional parameters relevant to oil immobilization.

Understanding how agglomerates form and influence oil mobility could enable manufacturers to extend shelf life, optimize texture, and reduce reliance on stabilizing additives and tropical solid fats, which, despite their functionality, are associated with negative health impacts [20].

2. Materials and Methods

2.1. Preparation of Hazelnut-Based Pastes

2.1.1. Material

2.1.1.1. Hazelnut Pastes, Hazelnut–Sugar Pastes, and Nougat Pastes (Laboratory Scale). Raw hazelnuts of Turkish origin were obtained from August Storck KG (Berlin, Germany) and contained 56%–69% w/w oil and 2.3%–3.0% w/w water. They were roasted in a convection oven at 142°C for 30 min. Powdered sugar with a particle size of $36.3 \pm 0.5\,\mu m$ (d_{50}) was purchased from Südzucker AG (Mannheim, Germany). Defatted cocoa powder with a fat content of 0.2% w/w and a particle size of $9.9 \pm 0.03\,\mu m$ (d_{50}) was acquired from Homborg finest food (Minden, Germany). Cocoa butter was obtained from August Storck KG (Berlin, Germany).

2.1.1.2. Nougat Pastes (Industrial Scale). The flakes used for nougat paste production were manufactured on an industrial scale by Wilhelm Reuss GmbH & Co. KG (Berlin, Germany). They consisted of sugar, roasted hazelnuts, cocoa powder, and sunflower oil with a total fat content of 22% w/w. The origin of the ingredients was unknown.

2.1.2. Methods. Hazelnut-based systems of increasing compositional complexity were produced and analyzed: pure hazelnut pastes, hazelnut–sugar pastes, and nougat pastes produced at both laboratory and industrial scales (Figure 1). Grinding technology, G, MD, and MT were varied.

2.1.2.1. Hazelnut Pastes and Hazelnut–Sugar Pastes. Pure hazelnut pastes and hazelnut–sugar pastes were produced using three grinding technologies—a cutter, a ball mill, and a three-roll refiner—at two intensities (Table 1, Figure 1). Pure hazelnut pastes consisted of 100% w/w nuts (a total fat content of 62% w/w), and hazelnut–sugar pastes contained 70% w/w hazelnuts and 30% w/w sugar (a total fat content of 42% w/w). Macroscopic images of these pastes are shown in Supporting Information 1: Figure S1.

Pastes ground by a cutter (Maschinenfabrik Seydelmann KG, Germany) were processed for 4 or 12 min at Level 2 (Table 1). For ball milling and roller refining, the solids were preground using a Thermomix TM6 (Vorwerk, Germany) for 5 min (Figure 1). The resulting mass was further refined using a ball mill (NETZSCH Trockenmahltechnik GmbH, Germany) with plastic beads (ZetaBeads, fraction 3.0–3.3 mm) for 25 min or 3 h at 650 rpm (Table 1) or a three-roll refiner (Bühler AG, Switzerland) operating at 6 bar in the first pass and 15 bar at the second pass (Table 1). Due to the high firmness of the mass, hazelnut–sugar pastes could not be obtained after 25 min of ball milling.

2.1.2.2. Nougat Pastes (Laboratory Scale). Nougat pastes produced on a laboratory scale contained 50% w/w sugar, 39% w/w roasted hazelnuts, 8% w/w cocoa butter, and 3% w/w defatted cocoa powder, resulting in a total fat content of 31% w/w. The pastes were produced at three levels of G, MT, and MD (Figure 1, Table 2).

A coarse grinding degree (G-coarse) was obtained by pregrinding the sample in a Thermomix for 5 min. A medium grinding degree (G-medium) was achieved after the first roller-refining pass at 6 bar, while a fine grinding degree (G-fine) was produced after the second roller-refining pass at 15 bar (Figure 1, Table 2). Macroscopic images of the flakes after grinding are shown in Supporting Information 2: Figure S2.

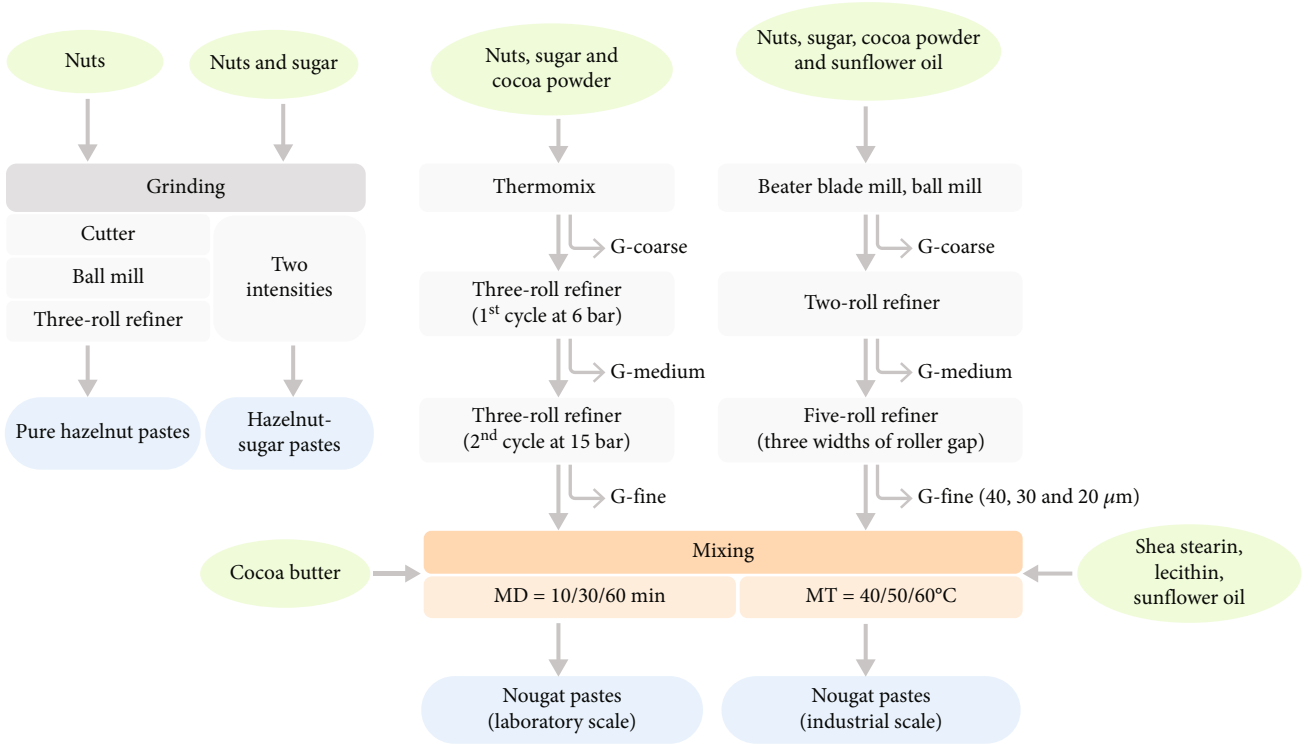

FIGURE 1: Production of hazelnut-based pastes with increasing matrix complexity: pure hazelnut paste (100% w/w nuts), hazelnut–sugar paste (70% w/w nuts and 30% w/w sugar), nougat paste produced on a laboratory scale (50% w/w sugar, 39% w/w nuts, 8% w/w cocoa butter, and 3% w/w cocoa powder), and industrially produced nougat pastes (49% w/w sugar, 18% w/w nuts, 17% w/w sunflower oil, 11% w/w cocoa powder, 4.5% w/w shea stearin, and 0.5% w/w lecithin). Grinding degree (G), mixing duration (MD), and mixing temperature (MT) were varied.

TABLE 1: Overview of pure hazelnut pastes and hazelnut–sugar pastes processed with different grinding technologies at two intensities.

Sample name	Symbol	Grinding technology	Grinding intensity
Cutter (4 min)	⬟	Cutter	4 min
Cutter (12 min)	⬟	Cutter	12 min
Ball mill (25 min)	▶	Ball mill	25 min
Ball mill (3 h)	▶	Ball mill	3 h
Roller refiner (1. Pass)	◆	Three-roll refiner	First pass (6 bar)
Roller refiner (2. Pass)	◆	Three-roll refiner	Second pass (15 bar)

Cocoa butter was pretempered to 40°C for 24 h and gently mixed with the flakes using a Thermomix in reversed mode at Level 1 with 100 min^{-1} for 10, 30, or 60 min (MD-10, MD-30, and MD-60) at 40°C, 50°C, or 60°C (MT-40, MT-50, and MT-60) (Figure 1, Table 2). The nougat pastes were filled in glass containers covered with aluminum foil, cooled down to 4°C for 24 h, and stored at 18°C. Macroscopic images of the nougat pastes are provided in Supporting Information 3: Figure S3.

2.1.2.3. Nougat Pastes (Industrial Scale). The industrially produced nougat pastes contained 49% w/w sugar, 18% w/w hazelnuts, 17% w/w sunflower oil, 11% w/w low-fat cocoa powder, 4.5% w/w shea stearin, and 0.5% w/w lecithin. The total fat content was 34% w/w. The pastes were produced at five levels of G and three levels of MD (Figure 1, Table 2).

Roasted hazelnuts were preground using a beater blade mill followed by a ball mill (G-coarse) (Figure 1, Table 2). Sugar, cocoa powder, and sunflower oil were added and then ground using a two-roll refiner (G-medium). Fine grinding was performed using a five-roll refiner (G-fine) at three-roll settings (parameters unknown), which resulted in typical particle sizes of approximately 40, 30, or 20 μm.

TABLE 2: Overview of nougat pastes produced on a laboratory and industrial scales at varying grinding degree (G), mixing temperature (MT), and mixing duration (MD). Bold text indicates the parameters that were varied.

Sample name	Symbol	Grinding technology and intensity	G(-)	MT (°C)	MD (min)
Nougat pastes (laboratory scale)					
G-coarse	●	Thermomix	**Coarse**	40	60
G-medium	●	Three-roll refiner (1. Pass)	**Medium**	40	60
MT-50	●	Three-roll refiner (2. Pass)	Fine	**50**	60
MT-60	●	Three-roll refiner (2. Pass)	Fine	**60**	60
MD-10	●	Three-roll refiner (2. Pass)	Fine	40	**10**
MD-30	●	Three-roll refiner (2. Pass)	Fine	40	**30**
G-fine, MT-40, MD-60	●	Three-roll refiner (2. Pass)	Fine	40	**60**
Nougat pastes (industrial scale)					
G-coarse	★/▲/⬢	Beater blade mill, ball mill	**Coarse**	40	**10/30/60**
G-medium	★/▲/⬢	Two-roll refiner	**Medium**	40	**10/30/60**
G-fine (40 μm)	★/▲/⬢	Five-roll refiner	**Fine (40 μm)**	40	**10/30/60**
G-fine (30 μm)	★/▲/⬢	Five-roll refiner	**Fine (30 μm)**	40	**10/30/60**
G-fine (20 μm)	★/▲/⬢	Five-roll refiner	**Fine (20 μm)**	40	**10/30/60**

The flakes were fattened with sunflower oil, molten shea stearin, and lecithin at 40°C and mixed gently for 10, 30, or 60 min (MD-10, MD-30, and MD-60) using a Thermomix in reversed mode at Level 1 with 100 min^{-1} (Figure 1, Table 2). The nougat pastes were filled in glass containers covered with aluminum foil, cooled down to 4°C for 24 h, and stored at 18°C.

2.2. Identification of Agglomerates at the Microscopic Length Scale

2.2.1. Size and Form of Particles and Agglomerates. The particle size distribution of sugar and deoiled cocoa powder was measured using a static laser light diffraction unit (Mastersizer 3000, software Version 2.15, Malvern Instruments Ltd., Worcestershire, United Kingdom). The particle refractive index was set to 1.56, and the dispersant refractive index was 1.38. The particles were assumed to be irregularly shaped, and Mie theory was applied. The samples were mixed 1:1 w/v with butanol, equilibrated to room temperature, and then introduced into the dispersing unit with butanol (99.4%, Sigma-Aldrich, Merck KGaA, Darmstadt, Germany) as the dispersant. The laser obscuration was adjusted between 6.6% and 9.9%. The stirring speed of the dispersion unit was 3000 min^{-1}. A waiting time of 120 s before starting the measurement was maintained to ensure that the particles were dispersed uniformly. The particle sizes of the 10%, 50%, and 90% percentile (d) were given. Samples were measured sixfold.

The morphology and size of agglomerates in all samples were analyzed using a light microscope (Morphologi G3, Malvern Panalytical GmbH, Kassel, Germany). For sample preparation, 1 g of nut paste was diluted with 20 mL of rapeseed oil. A drop of the dispersion was applied to a slide and covered with a cover slip. Magnifications of 2.5×–50× were taken. The measurement was carried out at least six times.

To also capture larger particles in hazelnut-based pastes, particle sizes were additionally measured using a micrometer screw gauge (Tesa Technology, Switzerland) after each grinding step. The measurement was carried out at least six times. However, micrometer screw and light microscopy measurements do not provide full particle size distributions, as both methods yield only localized, single-point observations.

2.2.2. NMR for Investigating Geometric Restriction of Oil Mobility in Agglomerates. To investigate the geometric restriction of oil within agglomerates after each grinding step, the translational mobility of the oil molecules was determined using pulsed field gradient–stimulated echo (PFG-STE) diffusion measurements. The experiments were performed on a 400 MHz wide-bore (WB) magnet equipped with AVANCE NEO electronics and a 5-mm DiffBB broadband gradient probe; the software TopSpin 4.1.1 controlled the experiments. The ^{1}H-NMR signal in the chemical shift range of 0–12 ppm was recorded and quantified as a function of the gradient amplitude (g). To process the diffusion data, a model based on the assumption that the oil is geometrically confined in spherical domains [21–23] was applied. The MCPR (Murday–Cotts–Packer–Rees) approach is typically used to determine droplet size distributions in emulsions, for example, [24], and has been successfully applied to the characterization of oleosomes in plant matrices (e.g., nuts) [25]. It allows, via a fit to the data, the calculation of a mean volume-weighted equivalent diameter ($d_{33,ed}$) and the distribution width σ_{MCPR} based on a

lognormal distribution. The resulting parameters were analyzed as a function of diffusion time (Δ) to draw conclusions about the presence of geometric restrictions of the oil's translational mobility due to agglomeration.

In addition, spatially resolved magnetic resonance imaging (MRI) measurements were performed to further evidence the existence of agglomerates. These experiments were performed on a 200 MHz Avance III HD spectrometer with a 20 mm MICWB-40 probe and maximal magnetic field gradients of up to 1.5 Tm^{-1}. The software ParaVision 6.0.1 was used for data acquisition and processing. A combined approach, magic angle spinning (MAS) NMR and ^{1}H-MRI, was applied to investigate whether mechanical stress (e.g., rotation) causes localized oil leakage from potential agglomerates [26]: RARE MR images were compared before and after mechanical stress (rotation at 15 kHz for 2 min in a 4-mm MAS rotor) of samples.

In order to capture mechanisms of oil mobility reduction, in particular, by altered interactions as a result of smaller particles and increased specific surfaces during grinding, the transverse relaxation rate R_2 was also measured spatially resolved. The multislice multiecho (MSME) pulse sequence allowed the spatially resolved determination of R_2 , while the signal decay of individual voxels was modeled by an exponential function. The measurement parameters are listed in Supporting Information 7: Table S1. NMR measurements were performed once per sample, and the device error of the HF-NMR system is specified as < 5%.

2.3. Impact of Agglomerates on Oil Mobility at the Macroscopic Length Scale

2.3.1. OBC. The OBC of all hazelnut pastes was determined by centrifugation. The centrifugation tubes were weighed before (m_A) and after the addition of about 15 g of nut paste (m_B). The filled tubes were centrifuged with a 3K30 centrifuge (Sigma, Osterode, Germany) for 30 min at 20°C. The rotational speed was 16,000 min^{-1}, and the relative centrifugal force was 2.75×10^4 g ($\approx 2.7 \times 10^5$ m•s^{-2}). Then, the supernatant was drained off for 1 h. The tubes with the remaining nut paste were weighed again (m_C) to calculate OBC with Equations (1) and (2). All measurements were performed in triplicate.

$$c_{\text{released oil}}\,(\%) = \frac{(m_B - m_A) - (m_C - m_A)}{(m_B - m_A)} \bullet 100, \qquad (1)$$

$$\text{OBC}\,(\%) = 100 - c_{\text{released oil}}. \qquad (2)$$

2.3.2. Rheology. The rheological properties of the nougat pastes were analyzed using a Rheometer Physica MCR 301 (Anton Paar, Ostfildern, Germany) with a heating mantle (H-PTD200, Anton Paar, Ostfildern, Germany).

2.3.2.1. Preparation of Nougat Paste Pellets. To ensure uniform samples, nougat pellets were prepared via a modified method based on Hubbes et al. [9]. Two grams of molten nougat was filled into self-made stainless steel molds (∅ 30 mm, 2 mm height) and frozen for 30 min at −20°C. Prior to the measurement, the frozen nougat pellet was placed on the measuring plate and pretempered to 25°C for 30 min. The measurements were performed in triplicate.

2.3.2.2. Storage Modulus (G') and Loss Modulus (G''). Amplitude and frequency sweeps were performed for all samples with a plate–plate geometry (PP25/TG) at a measuring gap of 1.7 mm. The measurements were carried out at 25°C.

An amplitude sweep was assessed to determine the linear viscoelastic region of the nougat pastes. The frequency was kept constant (10 Hz), while the deformation was changed between 0.001% and 100%. Frequency sweeps were executed within the linear viscoelastic region at a controlled deformation of 0.01% with frequency varying from 1 to 100 Hz. G' and G'' were computed from raw data. The measurements were performed in triplicate.

2.3.2.3. Yield Point. The yield point (τ_0) of the nougat pastes was analyzed at 40°C with a cone–plate geometry (CP50-1/TG-SN24742, $d = 0.1$ mm). The shear rate increased logarithmically from 0.01 to 100 s^{-1} to destroy the structure and then decreased from 100 to 0.01 s^{-1} to calculate the yield point using IOCCC2000 (Windhab model). The measurements were performed in triplicate.

2.3.3. Oil Separation During Storage. The nougat pastes produced on a laboratory scale were stored in glass containers at 23°C for 4 weeks. The separated oil was pipetted off after 1, 2, and 4 weeks and weighed. The measurement was performed in triplicate.

3. Results

3.1. Identification of Agglomerates at the Microscopic Length Scale

3.1.1. Size and Form of Particles and Agglomerates. Samples ground with a cutter (pure hazelnut pastes and hazelnut–sugar pastes), Thermomix, or beater blade mill (nougat pastes) showed the largest particle sizes (Table 3). Pastes ground by a ball mill or roller refiner displayed comparatively smaller particles. For all milling technologies, particle size decreased with increasing grinding intensity.

It should be noted that micrometer screw readings and light microscopic measurements represent single-point measurements and therefore do not reflect the overall particle size distribution.

Since the detection of agglomerates is essential for understanding oil immobilization, light microscopy was employed for their direct observation (Figure 2; Supporting Information 4: Figure S4, Supporting Information 5: Figure S5). Pure hazelnut pastes displayed individual particles but no agglomerates, independent of both grinding technology and intensity (Supporting Information 4: Figure S4A–C). Hazelnut–sugar pastes exhibited agglomerates of approximately 100 μm after the second pass of roller refining (Supporting Information 4: Figure S4F), whereas no agglomerates were detected following grinding with a cutter or a ball mill (Supporting Information 4: Figure S4D,E).

TABLE 3: Particle size ranges of hazelnut-based pastes with different grinding degrees (Gs), determined using a micrometer screw gauge ($n = 6$) and light microscopic images ($n = 6$). These measurements provide local particle estimates and therefore do not reflect the overall particle size distribution in hazelnut-based pastes.

Sample name	Particle size (μm)
Pure hazelnut paste	
Cutter (4 min)	5–700
Cutter (12 min)	5–400
Ball mill (25 min)	5–60
Ball mill (3 h)	5–20
Roller refiner (1. Pass)	2–40
Roller refiner (2. Pass)	2–25
Hazelnut–sugar paste	
Cutter (4 min)	5–750
Cutter (12 min)	5–400
Ball mill (25 min)	1–60
Ball mill (3 h)	1–20
Roller refiner (1. Pass)	1–30
Roller refiner (2. Pass)	1–20
Nougat paste (laboratory scale)	
G-coarse	5–800
G-medium	2–51
G-fine	2–12
Nougat paste (industrial scale)	
G-coarse	5–900
G-medium	5–150
G-fine (40 μm)	1–45
G-fine (30 μm)	1–32
G-fine (20 μm)	1–12

Agglomerate formation as a function of grinding intensity is shown in Figures 2a, 2b, and 2c exemplarily for laboratory-scale nougat pastes. While G-coarse and G-medium resulted in individual particles, agglomerates > 50 μm became visible in G-fine. In the industrially produced nougat pastes, agglomerates larger than 250 μm were observed in G-fine (Supporting Information 5: Figure S5A).

After the subsequent mixing step, agglomerates were no longer visible in light microscopy of hazelnut-based pastes, as exemplarily shown for MD-60 in laboratory-scale nougat pastes (Figure 2d) and in industrially produced nougat pastes (Supporting Information 5: Figure S5B).

Grinding technology and efficiency proved to be key factors in agglomerate formation. During the second pass of roller refining, smaller particles (approximately 1–25 μm, Table 3) with increased surface area, in combination with higher compression pressure, intensified particle–particle interactions [13, 27, 28]. In contrast, no such structures were observed in samples processed using a ball mill, cutter, Thermomix, or beater blade mill, which can be attributed to the different grinding forces acting on the material. Unlike a roller refiner, which operates predominantly through compression between the rolls, the cutter, Thermomix, and beater blade mill subject the material mainly to shear and impact forces, generating comparatively coarse particles that do not form a dense packing and, due to their lower specific surface area, exhibit weaker particle–particle interactions [13, 29]. In contrast, ball milling produced particle sizes comparable to roller refining (Table 3), yet no agglomerates were detected by light microscopy in any of the ball-milled samples. It is presumed that impact and compression forces acting within the ball mill temporarily promote agglomeration; however, these agglomerates are continuously disrupted by the mixing dynamics and motion of the grinding media [17, 30].

In addition to the processing conditions, the formulation itself had a significant impact on agglomerate formation. Agglomerates were only observed when additional solids such as sugar or cocoa powder were present (hazelnut–sugar and nougat pastes). This may partly be explained by the larger oil content of pure hazelnut pastes (~62% w/w) compared to hazelnut–sugar pastes (~42% w/w) and nougat pastes (laboratory scale: 31% w/w; industrial scale: 34% w/w), which reduces particle–particle interactions necessary for agglomeration [13]. Furthermore, nut particles alone may exhibit lower interparticle affinity or a reduced capacity to form stable agglomerates compared to sugar or sugar–nut combinations. The hydrophilic surface of sucrose promotes the formation of "sticky" surface films even at low residual moisture levels, thereby facilitating agglomerate formation [11, 31].

It is assumed that oil becomes entrapped within these agglomerates [12, 19]. This assumption is supported by the macroscopic texture of the nougat flakes, which changes from a wet, oily mass in G-coarse to a dry and crumbly texture in G-fine (Supporting Information 2: Figure S2).

The breakdown of agglomerates during mixing can be attributed to the shear forces acting on the material, which disrupt these structures [12] and indicate a pronounced shear sensitivity. This is in accordance with findings by Guckenbiehl et al. [19], who reported a decrease in OBC and viscosity of chocolate mass with prolonged conching. This observation is consistent with the fact that no agglomerates were detected in samples processed using a cutter, ball mill, beater blade mill, or Thermomix, as any agglomerates formed during grinding would be immediately destroyed by the integrated mixing action inherent to these technologies [16, 18, 29, 32]. Additionally, agglomerates may be partially disrupted by dilution in oil prior to microscopy, representing a methodological limitation.

3.1.2. NMR for Investigating Geometric Restriction of Oil Mobility in Agglomerates. The possible, finely dispersed storage of oil in interstitial spaces of agglomerates can be investigated by diffusion measurements and modeling using the MCPR approach. Unlike other methods for determining particle or droplet sizes, PFG-STE measurement allows the size of primary inclusions to be determined independently of any agglomeration into larger particles and without dilution. Therefore, the results may differ from those obtained by optical methods such as laser diffraction and lead to

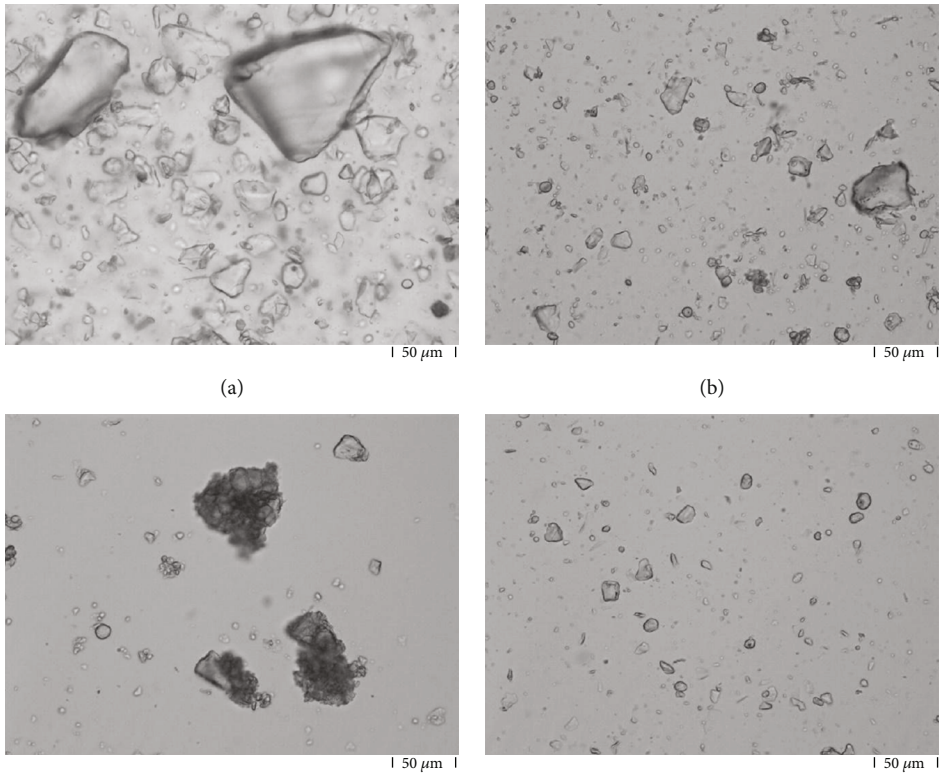

FIGURE 2: Light microscopy images of nougat pastes produced on a laboratory scale at 20× magnification. Presented are (a) G-coarse (after pregrinding using a Thermomix), (b) G-medium (after the first pass of roller refining at 6 bar), (c) G-fine (after the second pass of roller refining at 15 bar), and (d) G-fine after mixing for 60 min. Measured in six independent replicates; one representative example is shown.

smaller values of $d_{33,ed}$. The dependence of $d_{33,ed}$ on Δ provides information on how well the model describes the experimental data and consequently the reliability of the size distribution of the primary inclusions within the agglomerates. At the same time, it provides information about the geometric restriction of the oil molecules by the surrounding matrix. If $d_{33,ed}$ is independent of Δ, this indicates adequate modeling of closed, nearly spherical structures. If, on the other hand, $d_{33,ed}$ shows a dependence on Δ, this indicates that the oil molecules are confined, but not fully enclosed, for example as a result of interconnected micrometer-sized pores such as open pore systems. In addition, further length scales of compartment sizes may be present, or the geometry may deviate significantly from the spherical shape. In addition, the distribution width σ_{MCPR} gives insight into the size distribution of the restricting geometries.

For pure hazelnut pastes, $d_{33,ed}$ shows a pronounced Δ dependence across all grinding methods investigated (Figure 3a), indicating the absence of closed geometries in the oil phase, which is consistent with light microscopic images (Supporting Information 4: Figure S4A–C).

By adding sugar to the hazelnuts and then grinding them to hazelnut–sugar pastes, this dependence decreases significantly, especially in samples that were ground with a ball mill or by rolling (Figure 3c). The influence of the degree of grinding on the Δ dependence of $d_{33,ed}$ is clear: Smaller particle sizes lead to a smaller Δ dependence of $d_{33,ed}$. When rolled twice to a fine mass, $d_{33,ed}$ shows complete Δ independence within the measurement accuracy, which suggests the formation of closed agglomerate structures with entrapped oil, consistent with light microscopic images (Supporting Information 4: Figure S4D–F). Corresponding findings can also be observed in industrially produced nougat pastes (Figure 3e). With increasing degree of grinding, the Δ dependence decreases—agglomerate formation is assumed for samples with particle sizes $\leq 40\,\mu$m. σ_{MCPR} is approximately in the same size range of 0.5–0.8 μm.

In addition to evidence of agglomeration formation by rolling, the mass-related initial signal intensity $S_0 m^{-1}$ of the PFG-STE decays (Figures 3b, 3d, and 3f) indicates that not only the translational mobility of the oil was affected by inclusion but also its intrinsic mobility. When nuts and sugar are ground together by a ball mill or rollers, $S_0 m^{-1}$ is reduced by a factor of 10^2–10^4 compared to grinding without sugar, depending on the degree of grinding. The finer the grinding, the smaller $S_0 m^{-1}$. At a constant oil content in a comparable environment, $S_0 m^{-1}$ would be expected to be independent of the grinding technology. However, the observed signal reduction strongly indicates changes in the relaxation properties caused by finer grinding. Increased surface relaxation is likely to occur due to larger specific surfaces and smaller distances between particles and oil molecules.

For qualitative assessment of the oil distribution in finely rolled samples and to confirm the presence of oil in

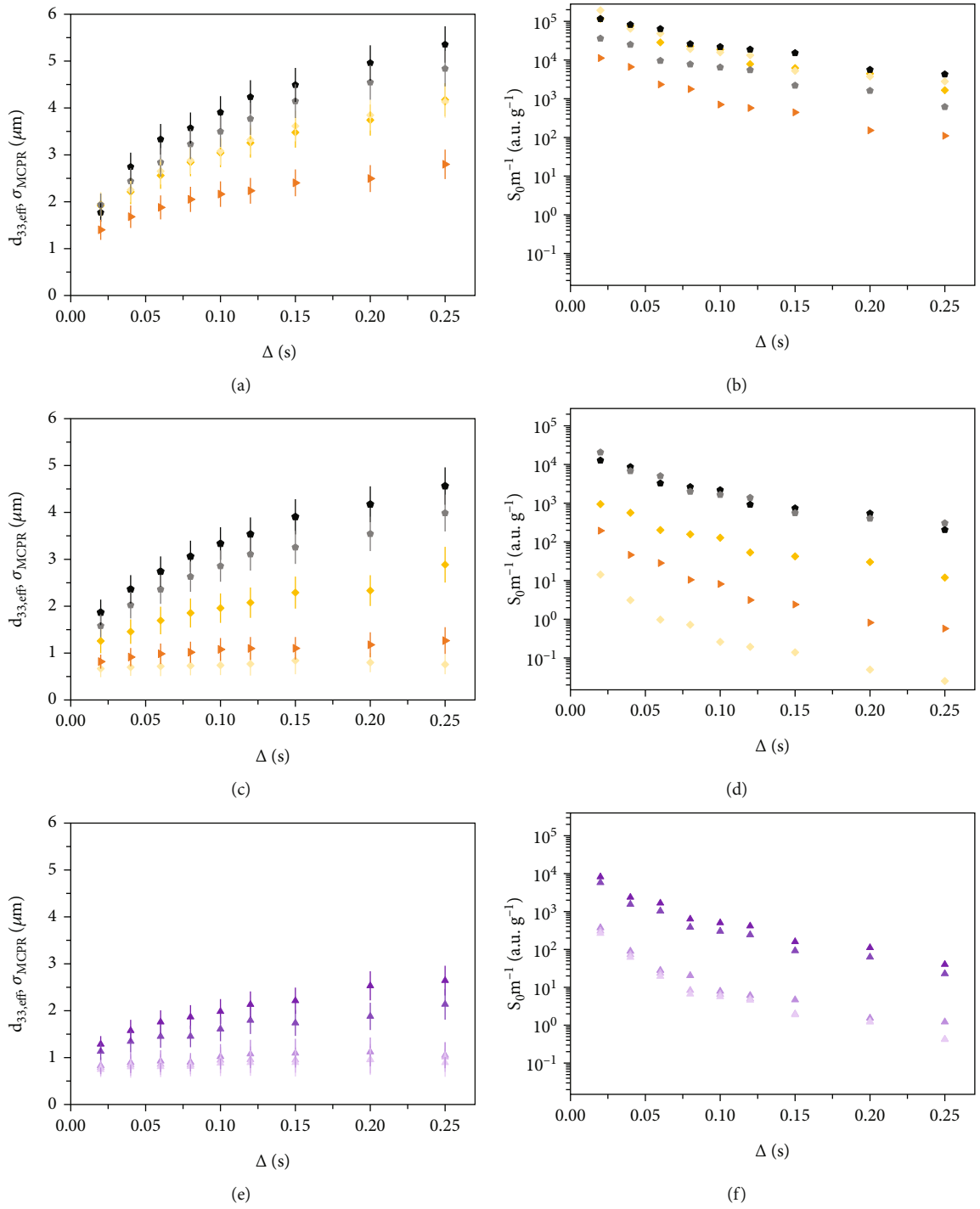

FIGURE 3: $d_{33,ed}$ and σ_{MCPR} (vertical lines) from PFG-STE diffusion measurements and modeling using the MCPR approach as a function of Δ for (a) pure hazelnut pastes, (c) hazelnut–sugar pastes, and (e) industrially produced nougat pastes. The mass-related initial signal intensity S_0m^{-1} of the PFG-STE diffusion measurements of (b) pure hazelnut pastes, (d) hazelnut–sugar pastes, and (f) industrially produced nougat pastes additionally indicates the reduction in the intrinsic mobility of the oil through the addition of sugar and increasing grinding. The measurements were performed in a single replicate.

agglomerate interstices—as detected by PFG-STE—samples were analyzed by MRI before (Figure 4a) and after (Figure 4b) rotation in an MAS rotor. Before rotation, an almost identical signal intensity S of approx. 10 a.u. was observed across the sample with a low signal-to-noise ratio. After rotation, a significantly larger signal intensity of approx. 65 a.u. was measured in the center of the rotor, indicating a mechanically induced separation of the oil from the agglomerate composite. In contrast, lower intensities (≈15 a.u.) were detected on the rotor wall, suggesting oil

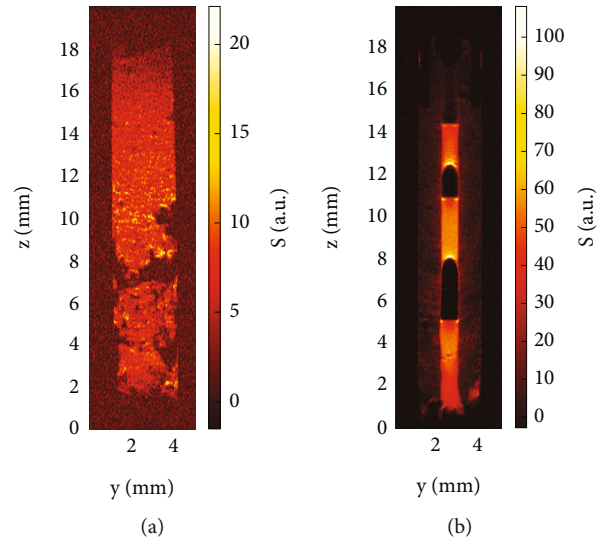

FIGURE 4: Rolled material in a 4-mm MAS rotor (a) before and (b) after "centrifugation" with locally larger signal intensity in the center of the rotor ($n = 1$). The contained oil separates from the other components, which indicates the presence of oil-filled spaces in the rolled material.

depletion. These observations prove that, despite the powdery nature of the sample, the oil in rolled material is still dispersed in the product and is not lost during the process. However, it can be released under mechanical stress. This supports the assumption of the existence of agglomerates with enclosed oil at particle sizes $\leq 40\,\mu$m.

The fact that a rather uniform signal intensity of approx. 10 a.u. was observed before rotation—about 6.5 times smaller than for pure oil—supports the hypothesis that the relaxation properties of the oil have changed due to increased surface relaxation as a result of grinding, which is reflected in the smaller $S_0 m^{-1}$ value. The signal intensity measured with R_2 weighting is significantly influenced by surface relaxation, which means that R_2 of the oil in the nut paste is larger than in the pure oil phase—with a correspondingly reduced signal intensity under identical measurement conditions of the RARE sequence.

The increase in surface relaxation as a result of finer grinding was quantified by measuring R_2 spatially resolved (Figure 5): R_2 increases with increasing degree of grinding of the components in nougat pastes (Figure 5a), while the signal amplitude of the continuous oil phase in nougat pastes remains almost constant (Figure 5b). The relaxation properties, but not the ^{1}H density, thus change depending on the degree of grinding. This can be attributed to increased surface relaxation due to the increase in particle surface of the solid components, which act as adsorption sites for oil. Finely ground pastes therefore exhibit a larger specific surface area and stronger oil interactions than coarsely ground pastes. Locally smaller R_2 values corresponding to those of hazelnut oil also indicate regional oil enrichments within the samples, suggesting that the material is inhomogeneous.

Overall, two mechanisms seem to overlap, leading to a reduction in oil mobility in finely rolled hazelnut–sugar or nougat pastes: firstly, the inclusion of oil in agglomerates and secondly, increased surface relaxation due to increased specific surface area and reduced interstitial spaces. The grinding process therefore leads to a reduction in both the intrinsic and translational mobility of the oil molecules in the pastes, which can be observed by NMR-based methods of diffusion and relaxation.

3.2. Impact of Agglomerates on Oil Mobility at the Macroscopic Level

3.2.1. OBC and Yield Point. Macroscopic tests provide indirect functional indicators for agglomerates and the stability of hazelnut-based pastes under varying processing conditions.

3.2.1.1. Pure Hazelnut Pastes and Hazelnut–Sugar Pastes. The OBC of pure hazelnut pastes decreased with increasing grinding intensity and was larger for a cutter compared to a ball mill or a roller refiner (Figure 6a). When 30% w/w sugar was added to the matrix (Figure 6b), samples showed similar OBC between the two grinding intensities; however, samples processed with a cutter exhibited a higher OBC. Due to the high firmness of hazelnut–sugar paste after 25 min of ball milling, the sample was not obtainable.

The results indicate that OBC of pure hazelnut pastes increases with larger particle sizes (Table 3), due to a higher proportion of intact oleosomes containing entrapped oil [33–35]. As pure hazelnut pastes contain only hazelnut particles and no sugar, the released oil had limited opportunities for entrapment within agglomerates or adsorption onto particle surfaces [11, 31]. In contrast, in hazelnut–sugar pastes, the oil released from oleosomes during refining becomes increasingly immobilized by sugar and hazelnut fragments through mechanical hindrance or particle–oil interactions [36]. In the case of roller-refined samples, the oil is presumably additionally entrapped within agglomerates composed of sugar and hazelnut particles, as evidenced by light

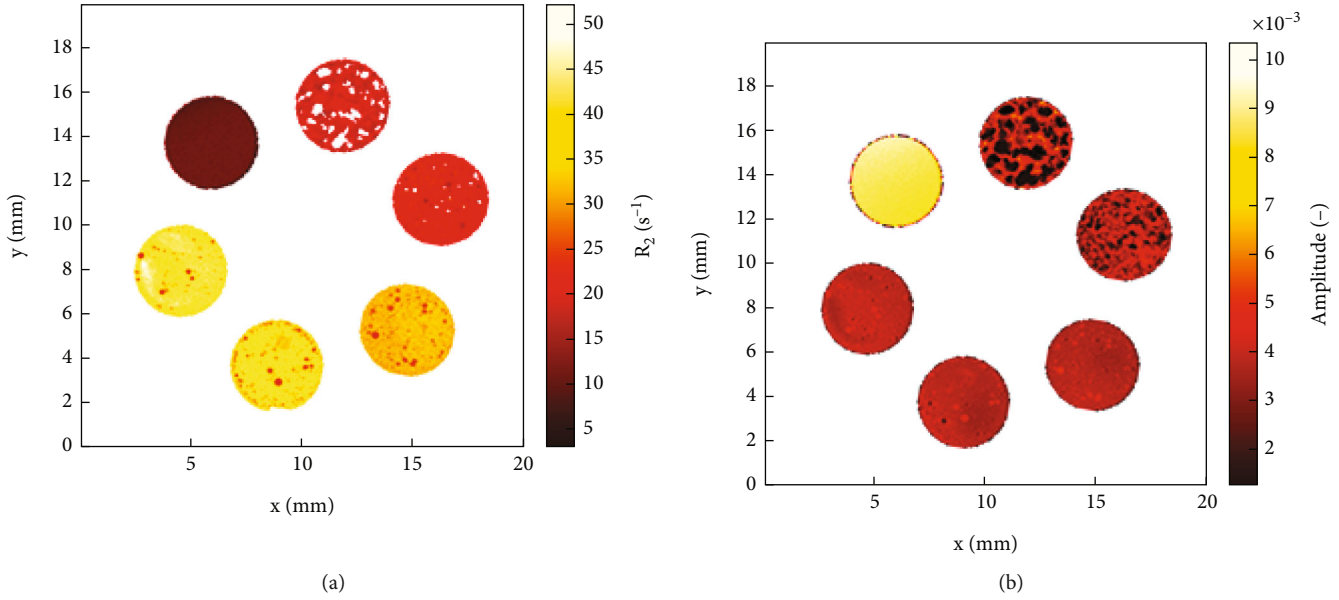

FIGURE 5: (a) R_2 image of industrially produced nougat pastes after various grinding steps. Conventional 5 mm NMR tubes were filled with the pastes. Starting with hazelnut oil as the reference oil with the smallest R_2 (5 s^{-1}), the grinding step increases clockwise ($n = 1$). R_2 shows differences between the nougat pastes and increases with increasing grinding step. In the white areas, R_2 was not analyzed due to the signal intensity being too low. (b) The corresponding signal amplitudes ($n = 1$): With the exception of hazelnut oil, the continuous phase of all samples shows a reduced, but similar signal amplitude ($\approx 3.5 \times 10^{-3}$). Data were fitted exponentially with spatial resolution.

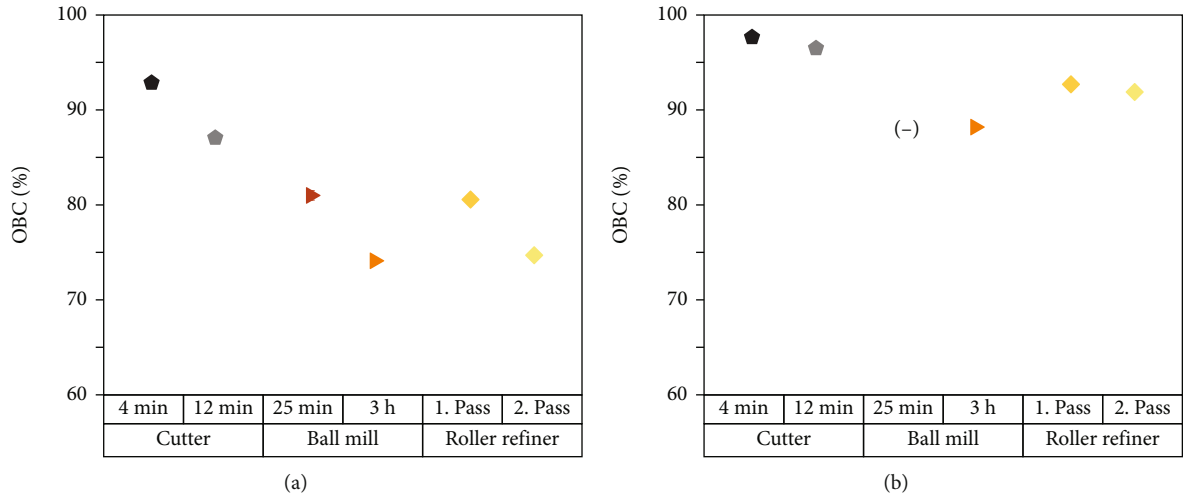

FIGURE 6: OBC of (a) pure hazelnut pastes and (b) hazelnut–sugar pastes with three grinding technologies (cutter, ball mill, or roller refiner) at two intensities. Values are expressed as mean with empirical SD of three replicates. The SD is in the order of the symbol size.

microscopy and NMR measurements (Figure 3; Supporting Information 1: Figure S1).

3.2.1.2. Nougat Pastes. Within the more complex matrix of nougat pastes, produced on both laboratory scale (Figure 7a,c) and industrial scale (Figure 7b,d), G-fine exhibited larger values for OBC and yield point compared to G-coarse, except for industrially produced G-fine (20 μm).

OBC and yield point of nougat pastes decreased with increasing MD (Figure 7), except for G-coarse (industrial scale), where MD had no measurable effect on the yield point.

In contrast to pure hazelnut pastes (Figure 6a), where finer grinding reduced OBC, nougat pastes showed the opposite trend (Figure 7). Both OBC and yield point increased with increasing grinding fineness, which is in accordance with the reduced oil mobility in finely ground hazelnut–sugar pastes and nougat pastes observed by NMR (Figure 3). This effect can be explained by the formation of agglomerates resulting from the presence of additional solids such as sugar and cocoa powder [11, 12, 31] and by the adsorption of released oil onto the surface of these particles. These mechanisms are promoted by the reduced particle size and the resulting increase in total surface area at higher grinding intensity [13, 36].

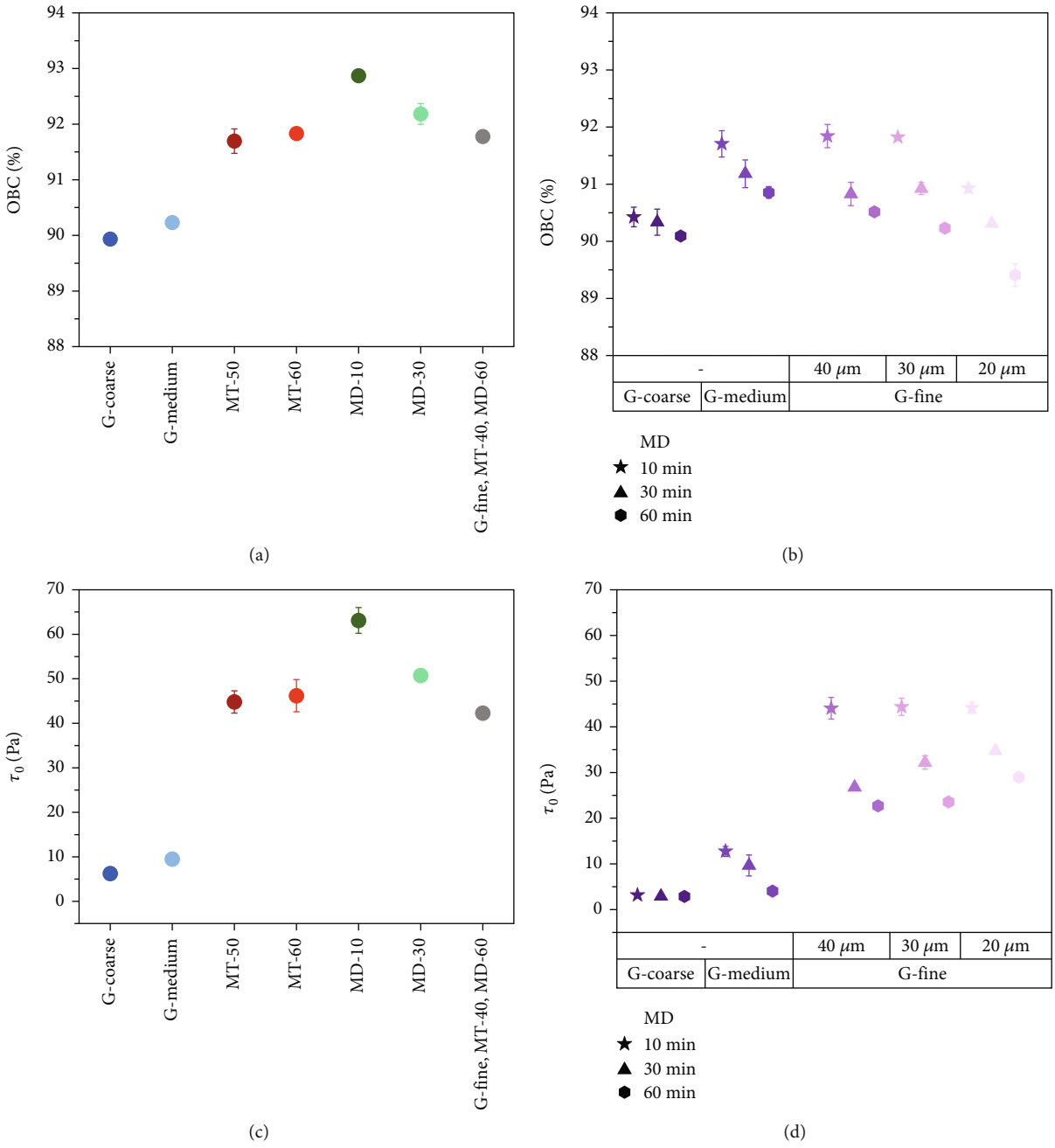

FIGURE 7: (a, b) OBC and (c, d) yield point (τ_0) of nougat pastes produced on a (a, c) laboratory scale and (b, d) industrial scale with varying grinding degree (G) (coarse, medium, and fine), mixing temperature (MT) (40°C, 50°C, and 60°C), and mixing duration (MD) (10, 30, and 60 min). The flow curves were evaluated according to the IOCCC2000 (Windhab model). Values are expressed as mean with empirical SD of three replicates.

However, a decrease in OBC was observed for the industrially produced nougat paste G-fine (20 μm) (Figure 7b). This may be due to the release of more oil from disrupted oleosomes during grinding than can be adsorbed onto particle surfaces or retained within agglomerates.

Additionally, the decrease of OBC and yield point with increasing MD suggests that shear forces during mixing disrupted agglomerates and released entrapped oil. Light microcopy images of laboratory-scale produced nougat pastes (Figure 2c,d) and industrially produced nougat pastes (Supporting Information 5: Figure S5) before and after mixing support this observation and are further substantiated by the unchanged yield point of G-coarse with increasing MD (Figure 7d) due to the absence of agglomerates before mixing (Figure 2a). These results are in accordance with findings by Guckenbiehl et al. [19], who reported a decrease in OBC and viscosity of chocolate mass with prolonged conching.

In summary, agglomerates formed especially during fine grinding of hazelnut-based pastes using a roller refiner in the

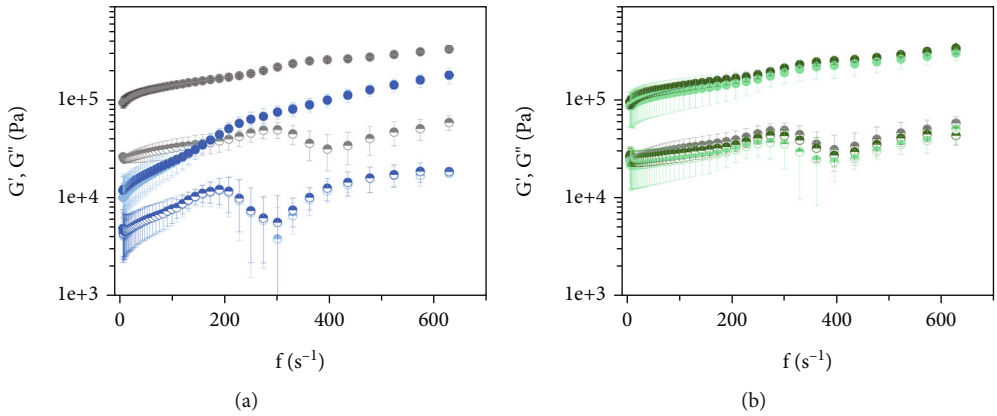

FIGURE 8: Viscoelastic behavior of nougat pastes produced on a laboratory scale with varying process parameters: (a) G-coarse (●), G-medium (●), and G-fine (●) and (b) MD-10 (●), MD-30 (●), and MD-60 (●). The measurements were performed within the linear viscoelastic region. The storage modulus (G') is marked by filled symbols and the loss modulus (G'') by half-filled symbols. Values are expressed as mean with empirical SD of three replicates.

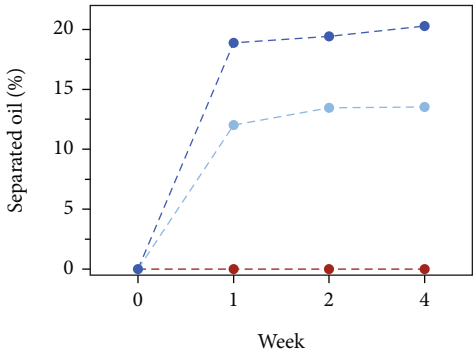

FIGURE 9: Relative percentage of separated oil (% w/w) on the surface of nougat pastes regarding their total fat content (33% w/w) over 4 weeks of storage. Nougat pastes were produced on laboratory scale with varying process parameters: G-coarse (●), G-medium (●), MT-50 (●), MT-60 (●), MD-10 (●), MD-30 (●), and G-fine, MT-40, MD-60 (●). Values are expressed as mean with empirical SD of three replicates. SD is in the order of the symbol size.

presence of additional solids such as sugar or cocoa powder. These substances contribute to oil immobilization and product stability, while their disruption through mixing leads to a decline in functional properties.

3.2.2. Viscoelastic Behavior. Amplitude sweeps of laboratory-scale nougat pastes (Supporting Information 6: Figure S6) revealed that the cross-over point occurred at lower deformations for G-coarse than for G-fine. For comparability across samples, a uniform deformation of 0.01% was selected for the subsequent frequency tests to ensure measurements within the linear viscoelastic region and to preserve the intact structural state of the pastes.

Nougat pastes exhibited larger G' and G'' for G-fine compared to G-medium and G-coarse within the linear viscoelastic region (Figure 8a). MD and MT had no effect on the viscoelastic behavior of the nougat pastes, as exemplarily demonstrated for the variation in MD (Figure 8b).

The enhanced viscoelasticity of G-fine aligns with their larger OBC and yield point, which can be attributed to the presence of agglomerates [12, 19] and adsorption of oil onto particles with a larger specific surface area [13, 36].

3.2.3. Oil Separation During Storage. The relative percentage of separated oil on the surface of laboratory-scale nougat pastes during 4 weeks of storage is shown in Figure 9. After 1 week, G-medium exhibited 12.0% ± 0.1% w/w surface oil separation, while G-coarse showed 18.9% ± 0.2% w/w. After 4 weeks, these values increased to 13.5% ± 0.2% and 20.3% ± 0.3% w/w, respectively. All finely ground nougat pastes (MT-50; MT-60; MD-10; MD-30; and G-fine, MT-40, MD-60) showed no visible oil separation on the surface even after 4 weeks of storage.

The absence of visible oil separation in all finely ground nougat pastes validates the results of other macroscopic, integral analyses—including OBC, yield point, and viscoelastic behavior—which indicated enhanced physical stability and oil immobilization in comparison to G-coarse and G-medium. These findings underline that macroscopic tests consistently reflect the stabilizing effect of agglomerates formed during fine grinding, supporting their functional relevance in oil immobilization and long-term product stability.

3.3. Correlation of Measurement Results on Different Length Scales. To comprehensively understand the formation and functional role of agglomerates in hazelnut-based pastes regarding oil immobilization, microscopic and macroscopic findings were correlated. The multiscale approach proved to reveal properties of both the direct detection of agglomerates on a microscopic level and the assessment of their technological relevance with macroscopic tests, thereby enabling a deeper understanding of structure–function relationships in hazelnut-based systems (Figure 10).

The presence of agglomerates was detected on a microscopic level using light microscopy and NMR diffusometry. In light microscopic images (Figure 2; Supporting Information 4: Figure S4, Supporting Information 5: Figure S5),

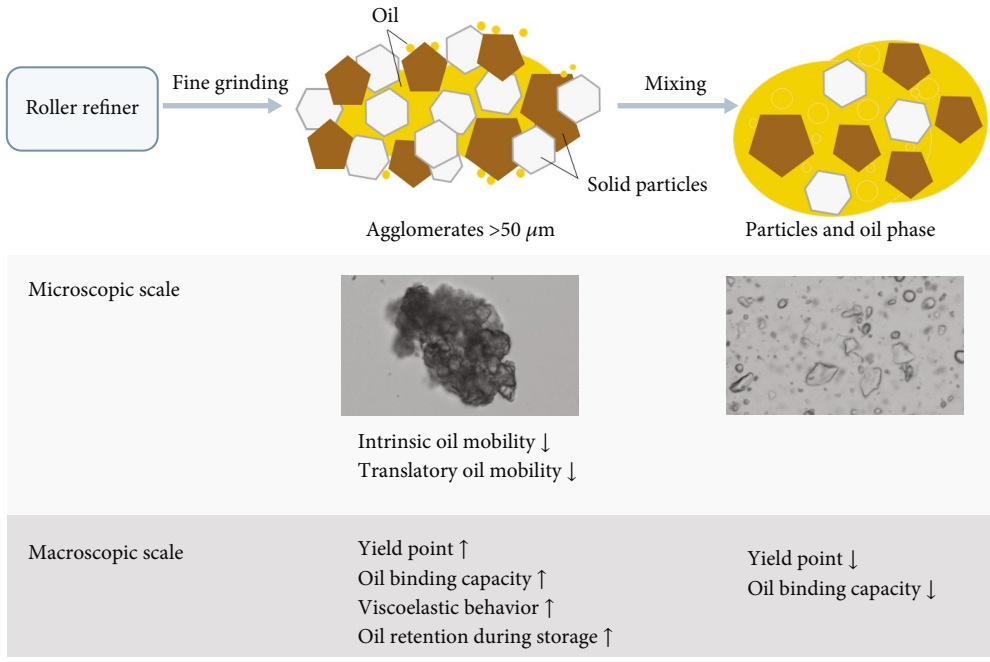

FIGURE 10: Schematic illustration of agglomerate formation during roller refining due to mechanical pressure, leading to oil entrapment within the structure (modified after Ziegleder [12]), and their subsequent disintegration during mixing, resulting in oil release. The relative sizes of the illustrated components are not on scale.

agglomerates were observed exclusively in finely ground hazelnut–sugar and nougat samples ground using roller refining, indicating that both additional solid particles such as sugar or cocoa powder and the grinding conditions are critical for agglomerate formation.

NMR diffusometry not only confirmed these findings but also revealed a reduction in intrinsic oil mobility in samples ground with a ball mill. This reduction may be attributed to three factors: (1) the small particle size—comparable to that achieved by roller refining—which results in a larger total surface area and thus increased oil adsorption; (2) the reduced interstitial spaces between small particles, which increase the tortuosity of diffusion paths; and (3) the formation of weakly cohesive agglomerates due to intensified particle–particle interactions. These agglomerates may have been disrupted during sample preparation for light microscopy (i.e., dispersion in oil), which could explain their absence (Supporting Information 4: Figure S4).

In contrast, cutter-processed samples with coarser particles exhibited larger oil mobility, consistent with the absence of agglomerates and limited surface contact between oil and solid particles.

Macroscopic, integral tests confirmed that agglomerate formation and particle size reduction contribute to enhanced oil immobilization and physical stability. In nougat pastes, OBC, yield point, and viscoelastic behavior increased with finer grinding and the presence of agglomerates, while oil separation during storage decreased. In contrast, pure hazelnut pastes (100% w/w nut) showed an inverse trend, with larger OBC for coarser particle sizes (e.g., after cutter processing), likely due to a larger amount of intact oleosomes.

The stability of agglomerates appeared to be sensitive to shear stress, as indicated by the decreasing yield point and OBC with increasing MD. This may also explain why no agglomerates were observed in light microscopic images of samples processed with a ball mill or cutter, as both technologies simultaneously grind and mix the mass, potentially disrupting agglomerates.

Overall, the impression—based on analyses on both length scales—is that two mechanisms overlap, leading to a reduction in oil mobility in finely rolled hazelnut–sugar or nougat pastes: the inclusion of oil in agglomerates and increased surface relaxation due to increased specific surface area and reduced interstitial spaces.

This combination of microscopic and macroscopic analyses allowed for a robust interpretation of how agglomerate structures influence the physical stability of the system and are affected by processing. Importantly, correlations between microstructural evidence and macroscopic indicators strengthen the assumption that agglomerates play a key role in oil immobilization. Relying on a single level of analysis would have been insufficient to capture the structural complexity and functional consequences of agglomerate formation and breakdown. The multiscale approach thus offers a valuable framework for investigating complex food matrices and for linking structural phenomena with technological functionality.

4. Conclusions

The impact of grinding technology and intensity, as well as mixing conditions on oil immobilization in hazelnut-based pastes, was studied across increasing compositional complexity—from pure hazelnut pastes to complex nougat systems—by combining microscopic and macroscopic

analyses to understand agglomerate formation and its functional implications.

Microscopic, spatially resolved analyses showed that agglomerates only formed under fine roller refining in hazelnut-based pastes containing additional solids, but not in pure hazelnut pastes. Light microscopy enabled the direct observation of agglomerates only in roller-refined samples, while NMR diffusometry additionally revealed a reduction in intrinsic oil mobility in ball-milled samples.

Macroscopic, integral analyses confirmed that agglomerates contribute to oil immobilization and product stability. In nougat and hazelnut–sugar pastes, fine grinding increased OBC, yield point, viscoelastic behavior, and long-term stability due to entrapment of oil in agglomerates and adsorption onto the larger surface area of smaller particles. Conversely, pure hazelnut pastes without added solids showed higher OBC with coarser grinding, likely due to a larger amount of intact oleosomes.

Overall, the results suggest that oil immobilization in hazelnut pastes results from two mechanisms: agglomerate entrapment and surface adsorption, both promoted by finer particle size and matrix composition. The multiscale approach proved essential for comprehensively studying the presence and functionality of agglomerates in nut-based pastes.

Agglomerates may represent an effective mechanism for immobilizing oil and thereby enhancing product stability. The findings indicate that roller refining to particle sizes below ~40 μm, in combination with gentle mixing due to the shear sensitivity of these agglomerates, is particularly suitable for promoting oil immobilization. Beyond hazelnut pastes, these insights enable a more general prediction of oil mobility and phase stability in diverse particle–oil dispersions and fat-based confectionery systems. Nevertheless, potential sensory implications associated with agglomerate formation should be taken into account and warrant investigation in future studies.

Nomenclature

OBC	oil binding capacity
TAGs	triacylglycerides
G	grinding degree
MD	mixing duration
MT	mixing temperature
σ_{MCPR}	distribution width
$d_{33,ed}$	mean volume-weighted equivalent diameter
g	gradient amplitude
Δ	diffusion time

Data Availability Statement

The data that support the findings of this study are available from the corresponding author upon reasonable request.

Conflicts of Interest

The authors declare no conflicts of interest.

Author Contributions

Hilke Schacht: writing—original draft, visualization, validation, methodology, investigation, and conceptualization; Lena Trapp: writing—original draft, visualization, validation, methodology, investigation, and conceptualization; Maike Föste: writing—review and editing, data curation, and conceptualization; Isabell Rothkopf: writing—review and editing, data curation, conceptualization, and project administration; Gisela Guthausen: writing—review and editing, writing—original draft, supervision, data curation, and conceptualization.

Funding

This work was funded by Bundesministerium für Wirtschaft und Klimaschutz (10.13039/100021130, 21785N). Open Access funding was enabled and organized by Projekt DEAL.

Acknowledgments

We thank the Chocolate Technology Working Group of the Industrial Association for Food Technology and Packaging (IVLV), Freising, Germany, for the joint discussion of experiments and results. We thank Kimberly Stahl and Valentin Haury for analytical assistance.

Supporting Information

Additional supporting information can be found online in the Supporting Information section.

Supporting Information 1. The supporting information provides additional data supporting the findings of the manuscript. It includes macroscopic images of the rolled material and final pastes, microscopic images, and particle size measurements. Furthermore, detailed parameters of the PFG-STE diffusion measurements are provided. Figure S1: Images of (A–F) pure hazelnut pastes and (G–K) hazelnut–sugar pastes ground by using (A, G) a cutter for 4 min, (B, H) a cutter for 12 min, (C) a ball mill for 25 min, (D, I) a ball mill for 3 h, (E, J) a three-roll refiner for one cycle at 6 bar, and (F, K) a three-roll refiner for an additional cycle at 15 bar.

Supporting Information 2. Figure S2: Flakes with varying grinding degrees for nougat paste production on a laboratory scale. Presented are (A) G-coarse (using a Thermomix), (B) G-medium (after one cycle of roller refining at 6 bar), and (C) G-fine (after the second cycle of roller-refining at 15 bar).

Supporting Information 3. Figure S3: Images of the final nougat pastes produced on a laboratory scale with varying grinding degrees (G-fine, G-medium, and G-coarse), mixing temperature (MT-40, MT-50, and MT-60), and mixing duration (MD-10, MD-30, and MD-60).

Supporting Information 4. Figure S4: Light microscopy images at 20× magnification of (A–C) pure hazelnut pastes (100% w/w nut) and (D–F) hazelnut–sugar pastes (30% w/w sugar and 70% w/w nut) after fine grinding using (A, D) a cutter, (B, E) a ball mill, or (C, F) a three-roll refiner.

Supporting Information 5. Figure S5: Light microscopy images at 20× magnification of industrially produced nougat pastes. Shown are (A) agglomerates formed in G-fine using a five-roll refiner and (B) their disruption after the subsequent mixing step (MD-60).

Supporting Information 6. Figure S6: Amplitude sweep used to determine the linear viscoelastic region of nougat pastes produced on a laboratory scale, shown exemplarily for (A) G-coarse and (B) G-fine. G' (filled symbols) and G'' (half-filled symbols) were recorded at 10 Hz, while strain was increased from 0.001% to 100%.

Supporting Information 7. Table S1: Measurement parameters of diffusion and MRI measurements for detecting agglomerates or interactions at the microscopic level.

References

[1] L. Principato, D. Carullo, G. Duserm Garrido, A. Bassani, R. Dordoni, and G. Spigno, "Rheological and Tribological Characterization of Different Commercial Hazelnut-Based Spreads," *Journal of Texture Studies* 53, no. 2 (2022): 196–208, https://doi.org/10.1111/jtxs.12655.

[2] S. Kıralan, A. Yorulmaz, A. Şimşek, and A. Tekin, "Classification of Turkish Hazelnut Oils Based on Their Triacylglycerol Structures by Chemometric Analysis," *European Food Research and Technology* 240, no. 4 (2015): 679–688, https://doi.org/10.1007/s00217-014-2371-0.

[3] L. Trapp, H. Schacht, L. Eymann, H. Nirschl, and G. Guthausen, "Oil Mobility in Hazelnut Oil-Based Oleogels Investigated by NMR," *Applied Magnetic Resonance* 54 (2023): 1445–1462, https://doi.org/10.1007/s00723-023-01571-6.

[4] E. J. Windhab, "Fluid Immobilization - A Structure-Related Key Mechanism for the Viscous Flow Behavior of Concentrated Suspension Systems," *Applied Rheology* 10, no. 3 (2000): 134–144, https://doi.org/10.1515/arh-2000-0009.

[5] J. Ampofo, F. S. Grilo, S. Langstaff, and S. C. Wang, "Oxidative Stability of Walnut Kernel and Oil: Chemical Compositions and Sensory Aroma Compounds," *Food* 11, no. 19 (2022): 3151, https://doi.org/10.3390/foods11193151.

[6] O. Aydemir, A. Beşir, and H. M. Aden, "Textural and Rheological Characteristics of Cocoa Hazelnut Cream Partially Substituted With Glucose Syrup," *European Food Science and Engineering* 2, no. 1 (2021): 13–17.

[7] B. Böhme, A. Bickhardt, and H. Rohm, "Pre-Crystallization of Nougat by Seeding With Cocoa Butter Crystals Enhances the Bloom Stability of Nougat Pralines," *Food* 10, no. 5 (2021): 1056, https://doi.org/10.3390/foods10051056.

[8] S.-S. Hubbes, A. Braun, and P. Foerst, "Crystallization Kinetics and Mechanical Properties of Nougat Creme Model Fats," *Food Biophysics* 15, no. 1 (2020): 1–15, https://doi.org/10.1007/s11483-019-09596-w.

[9] S.-S. Hubbes, A. Braun, and P. Foerst, "Sugar Particles and Their Role in Crystallization Kinetics and Structural Properties in Fats Used for Nougat Creme Production," *Journal of Food Engineering* 287 (2020): 110130, https://doi.org/10.1016/j.jfoodeng.2020.110130.

[10] B. Pajin, Đ. Karlović, R. Omorjan, V. Sovilj, and D. Antić, "Influence of Filling Fat Type on Praline Products With Nougat Filling," *European Journal of Lipid Science and Technology* 109, no. 12 (2007): 1203–1207, https://doi.org/10.1002/ejlt.200700044.

[11] E. O. Afoakwa, *Chocolate Science and Technology* (John Wiley & Sons, 2nd edition, 2016), https://doi.org/10.1002/9781118913758.

[12] G. Ziegleder, "Conchieren 1 - Sensorische, Technologische, Rheologische, Analytische Aspekte (Presentation)" https://zds-solingen.de/.

[13] G. R. Ziegler and R. Hogg, "Particle Size Reduction," in *Beckett's Industrial Chocolate Manufacture and Use*, eds. S. T. Beckett, M. S. Fowler, and G. R. Ziegler (John Wiley & Sons, 2017), 216–240, https://doi.org/10.1002/9781118923597.ch9.

[14] S. Vikharev, "Engineering of the Knife Grinding Machine Milling Process," *IOP Conference Series Materials Science and Engineering* 450, no. 3 (2018): 32020, https://doi.org/10.1088/1757-899x/450/3/032020.

[15] W. Xu, J. Wang, Y. Deng, et al., "Advanced Cutting Techniques for Solid Food: Mechanisms, Applications, Modeling Approaches, and Future Perspectives," *Comprehensive Reviews in Food Science and Food Safety* 21, no. 2 (2022): 1568–1597, https://doi.org/10.1111/1541-4337.12896.

[16] C. Alamprese, D. Datei, and Q. Semeraro, "Optimization of Processing Parameters of a Ball Mill Refiner for Chocolate," *Journal of Food Engineering* 83, no. 4 (2007): 629–636, https://doi.org/10.1016/j.jfoodeng.2007.04.014.

[17] C. F. Burmeister and A. Kwade, "Process Engineering With Planetary Ball Mills," *Chemical Society Reviews* 42, no. 18 (2013): 7660–7667, https://doi.org/10.1039/C3CS35455E.

[18] M. Fidaleo, S. Mainardi, and R. Nardi, "Modeling the Refining Process of an Anhydrous Hazelnut and Cocoa Paste in Stirred Ball Mills," *Food and Bioproducts Processing* 105 (2017): 147–156, https://doi.org/10.1016/j.fbp.2017.07.004.

[19] Y. Guckenbiehl, A. Martin, E. Ortner, et al., "Aroma-Active Volatiles and Rheological Characteristics of the Plastic Mass During Conching of Dark Chocolate," *Food Research International* 162, pt B (2022): 112063, https://doi.org/10.1016/j.foodres.2022.112063.

[20] M. Das and A. Das, "A Comprehensive Review on Strategies for Replacing Saturated Fats in Bakery Products," *Discover Food* 4, no. 1 (2024): 1–11, https://doi.org/10.1007/s44187-024-00240-2.

[21] J. S. Murday and R. M. Cotts, "Self-Diffusion Coefficient of Liquid Lithium," *Journal of Chemical Physics* 48, no. 11 (1968): 4938–4945, https://doi.org/10.1063/1.1668160.

[22] C. H. Neuman, "Spin Echo of Spins Diffusing in a Bounded Medium," *Journal of Chemical Physics* 60, no. 11 (1974): 4508–4511, https://doi.org/10.1063/1.1680931.

[23] K. J. Packer and C. Rees, "Pulsed NMR Studies of Restricted Diffusion. I. Droplet Size Distributions in Emulsions," *Journal of Colloid and Interface Science* 40, no. 2 (1972): 206–218, https://doi.org/10.1016/0021-9797(72)90010-0.

[24] R. Bernewitz, G. Guthausen, and H. P. Schuchmann, "NMR on Emulsions: Characterisation of Liquid Dispersed Systems," *Magnetic Resonance in Chemistry* 49 Suppl 1 (2011): S93–104, https://doi.org/10.1002/mrc.2825.

[25] L. Trapp, H. Schacht, H. Nirschl, and G. Guthausen, "Oleosomes in Almonds and Hazelnuts: Structural Investigations by NMR," *Frontiers in Physics* 13 (2025): 1494052, https://doi.org/10.3389/fphy.2025.1494052.

[26] T. Rudszuck, N. Schork, H. Nirschl, and G. Guthausen, "Nuclear Magnetic Resonance/Magnetic Resonance Imaging

on Lubricating Greases: Observation of Bleeding and Aging," *Magnetic Resonance in Chemistry* 60, no. 4 (2022): 452–462, https://doi.org/10.1002/mrc.5243.

[27] E. O. Afoakwa, A. Paterson, M. Fowler, and J. Vieira, "Microstructure and Mechanical Properties Related to Particle Size Distribution and Composition in Dark Chocolate," *International Journal of Food Science & Technology* 44, no. 1 (2009): 111–119, https://doi.org/10.1111/j.1365-2621.2007.01677.x.

[28] K. Franke, U. Bindrich, S. Schroeder, V. Heinz, and D. Middendorf, "Changes of Surface Properties of Sucrose Particles During Grinding in a Cocoa Butter-Based Suspension and Their Influence on the Macroscopic Behavior of the Suspension," *European Food Research and Technology* 250 (2024): 2353–2362, https://doi.org/10.1007/s00217-024-04542-8.

[29] A. Kumar and R. Yedhu Krishnan, "A Review on the Technology of Size Reduction Equipment," *International Journal of ChemTech Research* 13, no. 1 (2020): 48–54, https://doi.org/10.20902/ijctr.2019.130106.

[30] S. Rosenkranz, S. Breitung-Faes, and A. Kwade, "Experimental Investigations and Modelling of the Ball Motion in Planetary Ball Mills," *Powder Technology* 212, no. 1 (2011): 224–230, https://doi.org/10.1016/j.powtec.2011.05.021.

[31] C. Krüger, "Sugar and Bulk Sweeteners," in *Beckett's Industrial Chocolate Manufacture and Use*, eds. S. T. Beckett, M. S. Fowler, and G. R. Ziegler (John Wiley & Sons, 2017), 72–98, https://doi.org/10.1002/9781118923597.ch4.

[32] A. Borriello, N. A. Miele, P. Masi, and S. Cavella, "Rheological Properties, Particle Size Distribution and Physical Stability of Novel Refined Pumpkin Seed Oil Creams With Oleogel and Lucuma Powder," *Food* 11, no. 13 (2022): 1844, https://doi.org/10.3390/foods11131844.

[33] A. Barre, M. Simplicien, G. Cassan, H. Benoist, and P. Rougé, "Oil Bodies (Oleosomes): Occurrence, Structure, Allergenicity," *Revue Française D'allergologie* 58, no. 8 (2018): 574–580, https://doi.org/10.1016/j.reval.2018.10.005.

[34] S. Jokić, T. Moslavac, K. Aladić, M. Bilić, Đ. Ačkar, and D. Šubarić, "Hazelnut Oil Production Using Pressing and Supercritical CO2 Extraction," *Hemijska Industrija* 70 (2015): 43, https://doi.org/10.2298/HEMIND150428043J.

[35] C. Li, T. Dai, L. Deng, et al., "A Novel Whole Peanut Butter Refined by Stirred Media Mill: The Size, Microstructure, Rheology, Nutrients, and Flavor," *Journal of Food Science* 88, no. 9 (2023): 3879–3892, https://doi.org/10.1111/1750-3841.16688.

[36] H. Schacht, L. Trapp, M. Föste, I. Rothkopf, and G. Guthausen, "Oil Mobility in Sucrose-in-Oil Dispersions as a Function of Particle Morphology and BET Surface," *Food Research International* 203 (2025): 115797, https://doi.org/10.1016/j.foodres.2025.115797.